Journal of Civil Engineering and Construction 2020;9(3):138-149
https://doi.org/10.32732/jcec.2020.9.3.138

Evaluation of Normal Pressures during Filling in Steel Hoppers with Eccentric Outlet

Alireza Moazezi Mehretehran, Shervin Maleki

Department of Civil Engineering, Sharif University of Technology, Azadi Ave., Tehran, Iran
E-mail: a.moazezi@student.sharif.edu

Received: 24 May 2020; Accepted: 19 June 2020; Available online: 30 July 2020

Abstract: Filling pressures are a necessary starting point in the design of silos and hoppers. The hoppers with complicated geometries are common in industrial applications due to physical space constraints and the need to interface with other processing equipment. The current paper deals with the effect of outlet eccentricity on normal pressures formed in steel hoppers during distributed filling process. Using finite element method, progressive filling process in hoppers was simulated and by changing the percentage of outlet eccentricity, the variation of pressure distribution was fully studied. The results showed an increase in the normal pressures of shallow side compared with the steep side of eccentric hopper. To quantify the pressure asymmetry, two parameters were introduced and they were evaluated for practical range of material parameters and steel hoppers dimensions. The results obtained are of interest since they facilitate the design of silos and hoppers with eccentric outlet.
Keywords: Eccentric hopper; Progressive distributed filling; Normal pressure; Finite element method; Parametric study.

1. Introduction

Silos and hoppers are widely used for the storage and handling of bulk solids in industry. Hopper is an important part of storage vessels and normally supports the majority of loads induced by the particulate solids [1]. Three distinct phases exist in a silo or hopper work cycle: filling, storage and discharge. The filling condition is normally used as the reference state against which discharge pressures during flow are predicted [2–5] and a clear description of this phase is therefore vital, even for studies of discharge.

The hoppers with complicated geometries are common in industrial applications due to physical space constraints and the need to interface with other processing equipment. Owing to some particular needs, eccentric hoppers are also being widely used. One of the main advantages of the eccentric hopper, especially evident in small to midsize silos, is that it allows the discharge of the silo contents to a much more easily accessible location away from the silo body.

The first attempts in predicting the pressures developed in the wall of silos dates back to theoretical approach of Janssen [6]. This analysis was extended to the cases of conical and wedge-shaped hoppers by different authors [7–10]. Most of them used “The Method of Differential Slice” [11], but afterwards each made different assumptions concerning the evaluation of the ratio of wall pressures to vertical pressures. In predicting the wall pressures, “The Method of Characteristics” developed for plane strain situations [11,12] and the proposed theory that the pressure distribution near the apex of the hopper is in the form of a “Radial Stress Field” [13–16] are among the other theoretical approaches taken.

In addition to classical theories on this topic, with the advent of more powerful computers, numerical methods have become very useful in research on behavior of bulk solids. Numerical methods are very economical and lend themselves to comprehensive parametric studies. In this paper, the finite element method (FEM) is the primary approach.

Notably, the majority of past researches into hopper wall pressures have focused on concentric shaped hoppers. Both filling [1,3,17,18] and discharge [19–26] phases of circular cross-sectional hoppers have been addressed in these researches. A number of studies have also been conducted on pressures developed in silos with eccentric hoppers [27–33], but none of them have considered the aspects investigated in this paper.

In the present study, using the finite element analyses, efforts are made in assessment of normal pressures developed in steel hoppers with eccentric outlet during the filling phase. An advanced computational technique for simulating the progressive filling method [1,3,17,33,34] is used. The commercial software ABAQUS [35] is employed for the nonlinear finite element analyses. To date, as far as the literature survey shows, there is no such 3D modeling that specifically investigates the hopper body. The asymmetry of developed pressures is fully

addressed. The overpressure factor (OPF) in accordance to outlet eccentricity, as the peak pressure deviates from that of concentric counterpart, is defined. Considering the same concept, but for minimum pressure deviation from concentric hopper wall pressure, the reduction pressure factor (RPF) is also introduced. To expand this concept for further application, a parametric study on OPF and RPF values for practical range of material parameters and hoppers dimensions is conducted. Therefore, the main novelties of the paper would be summarized as follows:

1) Considering a comprehensive 3D modeling of eccentric hopper body and simulating a realistic progressive filling process.

2) Quantifying the eccentricity effects on normal pressure deviation from that of centered-outlet hopper by means of OPF and RPF values.

3) Conducting a parametric study for practical range of material parameters and steel hopper dimensions to better predict the OPF and RPF values.

2. Numerical modeling

2.1 Hopper geometry and eccentric outlet

To investigate the effect of eccentricity on variation of normal pressures in hopper body, a 3D conical sample hopper shown in **Figure 1** was assumed as the basic scheme. A 2D axisymmetric counterpart of that hopper was previously studied in Ref. [1]. Same dimensions were used to make it possible to compare results for the case of hopper with central outlet. This subject is explained further in section: "2.4 Additional points in modeling" below. Therefore, a total height of 2355.85 mm and a fixed diameter of 2400 mm and 400 mm for the largest and the smallest cross section of hoppers were considered, respectively. Similarly, a uniform hopper wall thickness of 6 mm was assumed. Note that, a smaller thickness (t=0.5 mm) was also examined in finite element models but the results remained unchanged.

The outlet was moved rightward to create eccentricity as presented in **Figure 2**. For the sake of consistency with the European Standard [36], the eccentricity was defined in terms of the ratio between the amount of outlet offset from centerline (e) in conical hopper to the largest diameter (D) in the same hopper. According to hopper dimensions, the ratio varies from zero to almost 0.416 which is defined as full eccentricity in the current paper. In the case of full eccentricity, the outlet is located in a way that a vertical wall segment is produced.

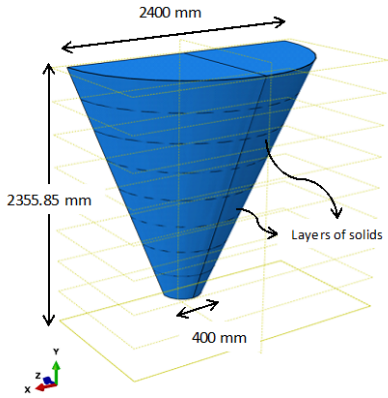

Figure 1. Basic scheme of 3D conical sample hopper.

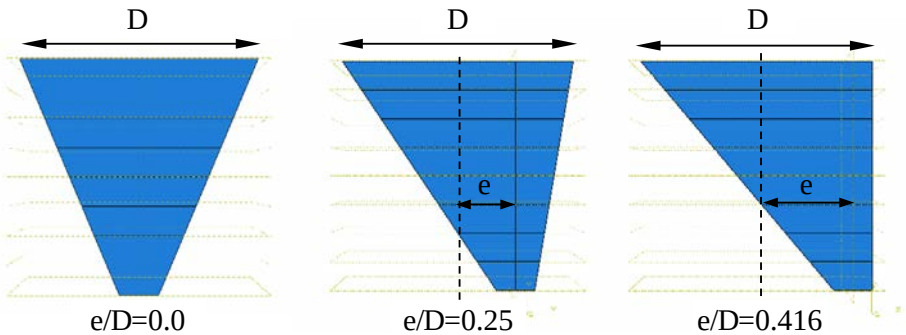

Figure 2. Definition of hopper eccentricity.

2.2 Filling method and guide lines for pressure assessment

According to the method of filling used, an almost flat top surface or a conical pile of particulate solids can be produced. Distributed filling of granular materials and pneumatic filling of powders are of the filling methods which result to flat top surface [17,36–38]. On the contrary, concentric or stream filling method causes materials to pile up and make a conical surface [1,37,38]. In the finite element models of this paper, the main focus is on the distributed filling method.

In the finite element simulation, several filling methods have been proposed such as, switched-on filling method, progressively increasing the density of the material or incremental layered filling with a small preloading in the material [20,39]. In a real filling process, the volume of the stored material is increasing. The boundaries of volume are changing continuously and hence their contact interactions. Accordingly, in the present study, the more sophisticated progressive filling method was used to simulate the process in 3D.

To implement progressive filling in the software, the final geometry of solid materials was partitioned into horizontal layers. Each layer comprised loading, contact interaction and material properties. Each layer landed on a body of material that was already stressed and hence was already deformed. This method led to a more realistic modeling of filling phase and is regarded as an advanced approach in 3D FEM to simulate the hopper filling.

To clarify the different set of points used for normal pressures reading in 3D finite element model, guide lines were defined as: Left, Right, Ring-2, Ring-3 and Ring-6, and are depicted in **Figure 3**. As will be shown later, these guide lines are useful in pressure study of sample hoppers, since practically the highest and the lowest normal pressures can be tracked almost along them.

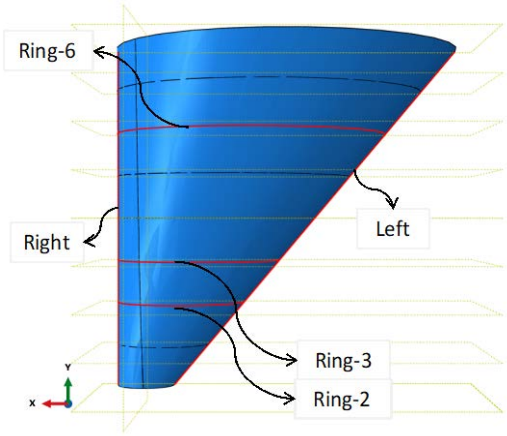

Figure 3. Guide lines used for normal pressures evaluation.

2.3 Finite element modeling

The 3D finite element analyses employed a Lagrangian frame of reference to represent both the hopper structure and its stored material. The hopper wall was modeled as a 4-node doubly curved thin shell element (S4R). The ensiled material was represented by an 8-node linear brick element (C3D8R). Both types of elements use reduced integration and hourglass control. For the sake of symmetry, only half of the hopper and bulk solids were generated for each analysis. The hopper structure was constrained in three principal directions of global coordinates system at the top edge. The stored solids were constrained in the same manner at the outlet boundary, corresponding to a closed outlet. The symmetry boundary conditions were applied in the plane of symmetry as well. Loading was applied by introducing uniform gravitational force to stored solids.

The surface-to-surface contact interaction accompanied by penalty method under contact pair algorithm was implemented as the mechanical contact simulation of bulk solids and hopper wall. The stick-slip behavior of wall and the stored solids were implemented through a single value (μ=0.5) for the wall friction coefficient using the Coulomb friction model available in the software for the tangential behavior. Moreover, hard contact simulated the normal behavior.

The material properties for hopper wall and granular material were similar to those of Ref. [1]. In this respect, the hopper was modeled by elastic properties of steel and an ideal elastic-plastic Drucker-Prager material with kinematic hardening was adopted for the bulk solids. A number of previous studies have been successfully adopted Drucker-Prager criterion for material modeling on the same issue [1,17,21–23,27,28,30–33,40]. However, the numerical predictions have shown that the adopted constitutive model for stored solids has little effect on the filling pressures [2,3,18,41]. Properties and parameters used for materials in the analyses are summarized in **Table 1**.

Table 1. Material properties used in FEM adopted from Ref. [1].

Steel hopper	Elasticity	Young's modulus	2.0×10^{11} Pa
		Poisson's ratio	0.3
Bulk solids	Elasticity	Young's modulus	5.5×10^{5} Pa
		Poisson's ratio	0.3
		Density	1000 kg/m^3
	Drucker-Prager plasticity	Angle of friction	55°
		Flow stress ratio	1
		Dilation angle	35°
		Drucker-Prager hardening (true stress (Pa) and strain)	50000,0 55000,0.02 60000,0.025 70000,0.03 120000,0.035

2.4 Additional points in modeling

A static nonlinear analysis was used to include nonlinear behavior of the granular materials. To establish verification for the procedure adopted in the present research (i.e., the progressive method in 3D environment), the hopper studied in Ref. [1] was adopted as the benchmark. In this regard, a 3D model of concentric hopper with conical pile at top surface which resembled the 2D axisymmetric counterpart of the benchmark hopper was modeled. **Figure 4a** shows the normal pressures developed in 3D model using both progressive and the more conventional switched-on filling method. In the latter method, gravity is applied in a linearly increasing manner for the entire mass of stored particulate solids during the span of loading time. A comparison of the results obtained with those of benchmark, as represented in **Figure 4b**, indicated that great consistency has been achieved in 3D modeling.

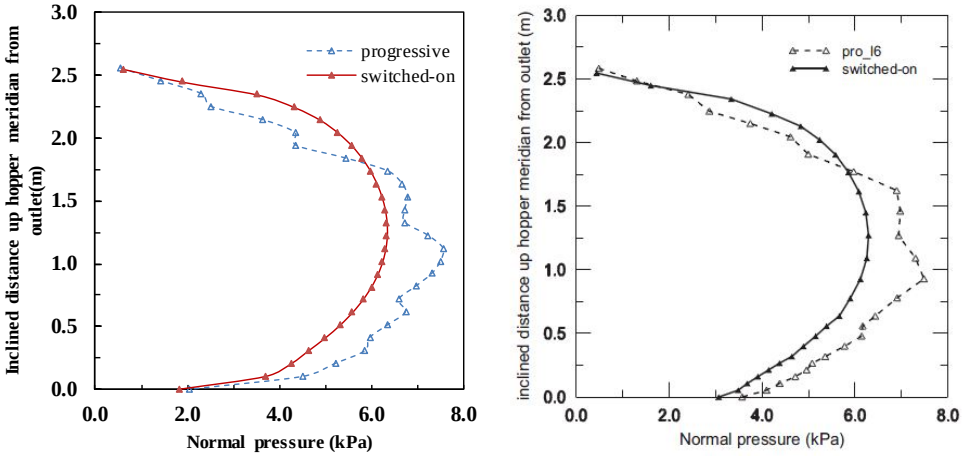

(a) **(b)**

Figure 4. Normal pressures developed on hopper wall calculated from: (a) 3D model of this paper, (b) 2D axisymmetric model by Ref. [1].

Additional aspects of modeling are described herein. First of all, the effect of number of layers in progressive filling method was explored. Regarding the hopper dimensions, almost stable distribution of pressures was achieved by 8 layers of bulk solids. For the hoppers with almost similar dimensions, 6 and 8 layers has been selected by previous studies [1,3,17,34]; hence 8 layers were picked in all analyses of this paper.

The other significant topic in granular materials modeling is that how the selected constitutive law may influence the final outputs of analyses. Due to small strains in filling phase [42] and considering the low pressure level in the hoppers without surcharge, the bulk solid exhibits almost elastic behavior. The apparent cohesion also plays an important role in this issue. In the present study, the hardening rule of Drucker-Prager criterion takes into account the apparent cohesion. For the range of apparent cohesions recommended for granular agricultural materials used in silo design [40,43], in the filling phase, the elastic behavior is dominant and plastic parameters have minor effect. Due to the same reasons, similar analyses with lower internal angle of friction (e.g. 20, 30 and 40 degrees) made negligible changes in the results.

Frictional tractions, in all analyses, can be related to normal pressures by means of mobilized wall friction coefficient, as recommended in the European Standard [36]. It is calculated considering the inclination of hopper wall segment along guide lines Left and Right. The frictional tractions outputs were examined and relatively close agreements were obtained in all cases. Although some recent studies have assessed the mobilized wall friction coefficient in steep and shallow hoppers [1,3,34], more detailed investigations on this issue could be undertaken in future researches.

3. FEM results and discussion

3.1 Normal pressures along guide lines

The predictions of normal pressures on the hopper wall under different eccentricities are shown in **Figure 5** along guide lines Left and Right. It is obvious from this figure, as the eccentricity grows the asymmetry in normal pressures take place. The results show an increase in the normal pressures of shallow side compared with the steep side of eccentric hopper. Due to slight discontinuities associated with reactivating new layers during progressive filling process, general form of pressure curves is not smooth.

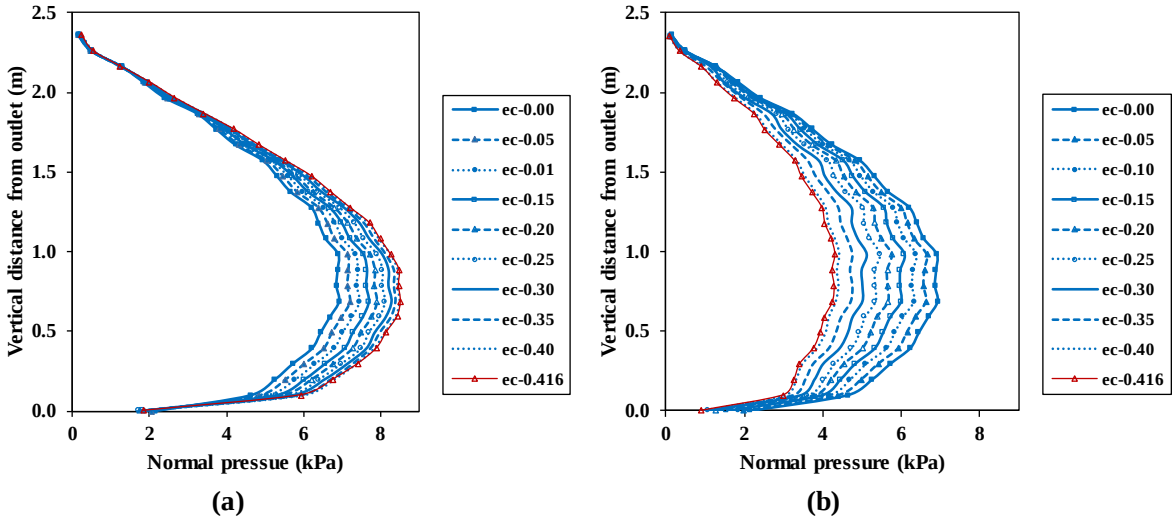

Figure 5. Normal pressure distribution for different eccentricities: (a) along Left, (b) along Right guide line.

To quantify the eccentricity effects on normal pressure deviation from that of centered-outlet hopper, two factors were defined as follows: (a) OPF; and (b) RPF. Due to defined geometry, the OPF and RPF are related to Left and Right guide lines, respectively. Note that, the design of wall thickness is based on the peak pressures obtained. Therefore, the introduced factors for each eccentricity were calculated by dividing the maximum value of normal pressure in eccentric hopper to the corresponding value in concentric one at the same elevation and point. **Table 2** represents the OPF and RPF values obtained for the sample hopper.

Table 2. OPF and RPF values determined for different amounts of eccentricity.

Model Number	*e/D*	OPF	RPF	Difference (OPF-RPF)
1	0	1.00	1.00	0.00
2	0.05	1.04	0.96	0.08
3	0.1	1.08	0.92	0.16
4	0.15	1.11	0.88	0.23
5	0.2	1.14	0.83	0.31
6	0.25	1.17	0.79	0.38
7	0.3	1.20	0.74	0.46
8	0.35	1.21	0.68	0.53
9	0.4	1.23	0.64	0.59
10	0.416	1.23	0.62	0.61

Investigation of normal pressure distribution along circumferential path defined under the title of Ring-2, Ring-3 and Ring-6 is also conducted. The results in **Figure 5** indicate that the maximum pressures along both Left and Right guide lines occurred between 0.5 and 1 meter from outlet in elevation of the sample hopper. Therefore, the

circumferential guide lines Ring-2 and Ring-3 with vertical coordinates of 2/8 and 3/8 of total height of hopper were considered, respectively.

To examine the circumferential pressure distribution in the upper part of sample hopper, Ring-6 with vertical coordinates of 6/8 of total height of hopper was additionally picked. **Figure 6** shows the normal pressures variation along these lines. The horizontal axes of these figures is the angle θ measured counter-clockwise as shown in **Figure 7** and is compatible with the European Standard [36] notation. General form of pressure curves in **Figure 6**, which take the schematic shape like **Figure 7** in polar coordinates, may be approximated by two cosine waves.

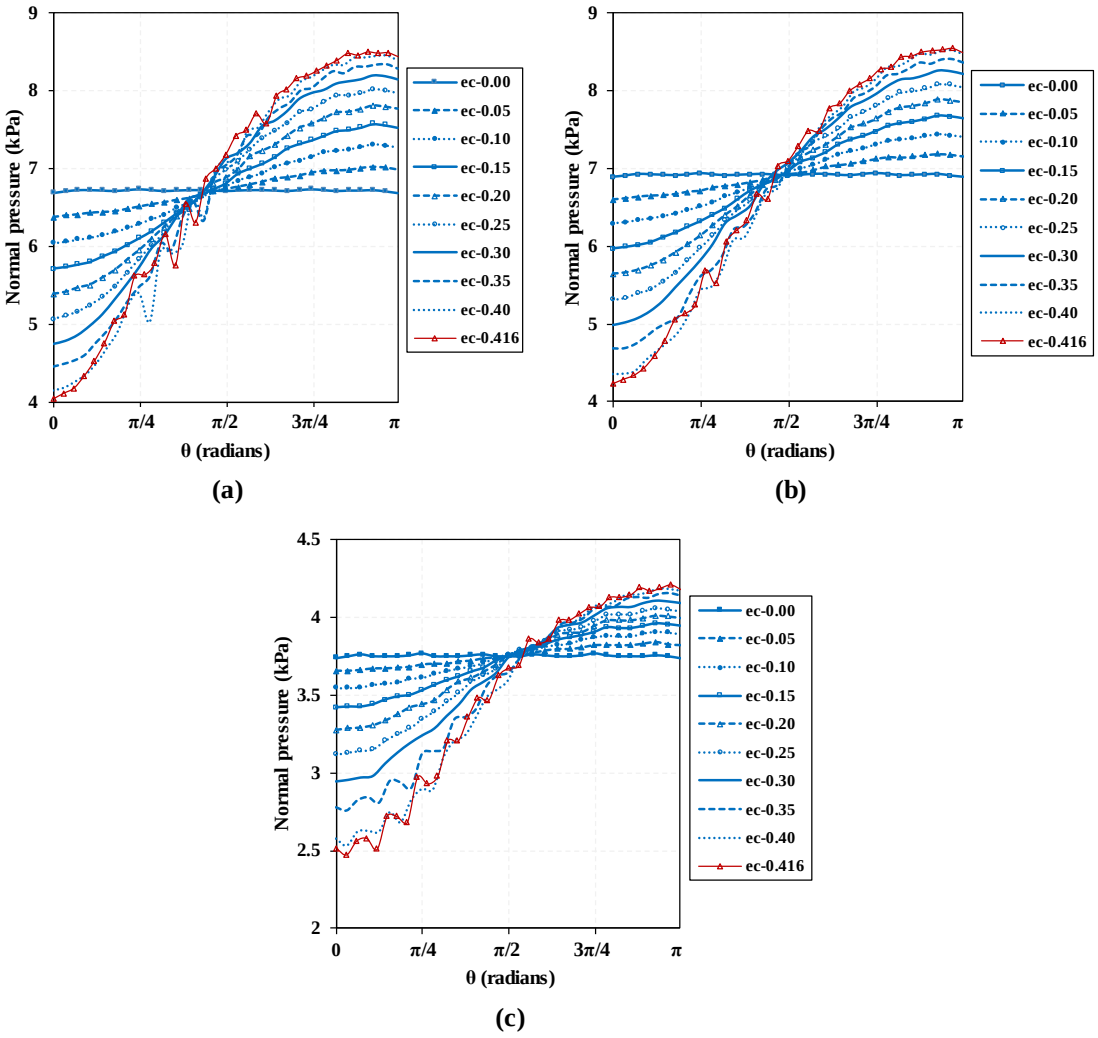

Figure 6. Normal pressure distribution: (a) along Ring-2, (b) along Ring-3 and (c) along Ring-6.

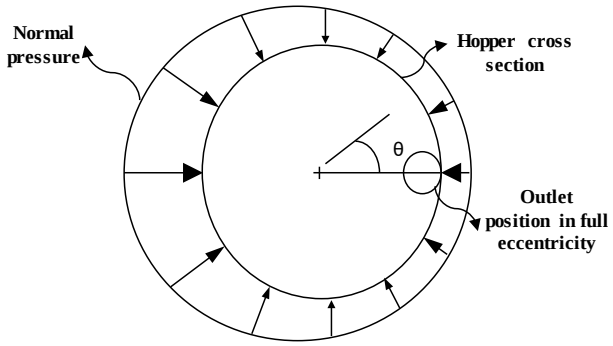

Figure 7. Schematic view of normal pressures in horizontal plane of hopper in polar coordinates.

All curves in **Figure 6** pass from a common point at almost $\pi/2$ radians along x-axis which intersects with the value of concentric normal pressure at the same elevation. Zero and π radians correspond to Right and Left guide lines in the plan view, respectively. For eccentric hoppers from 0 to $\pi/2$ radians in x-axis direction, the normal pressure is less than amount of concentric pressure at the same elevation. From $\pi/2$ to π radians, the normal pressure increases and its peak value is at π radians. This is consistent with the way that OPF and RPF values were defined.

3.2 On refinement of OPF and RPF values

To clarify the general effects of modeling parameters on OPF and RPF values, some more analyses were conducted. In the current section, 4 different amount of outlet eccentricities (i.e., e/D = 0.1, 0.2, 0.3 and 0.416) were used for parametric study. It was mentioned that in the filling phase the adopted constitutive model for stored solids has little effect on pressure predictions [2,3,18,41]. Consequently, the Drucker-Prager criterion parameters kept unchanged in further analyses.

One of the key features of bulk materials is Young's modulus (E). For the range of normal pressures exerted on the ensiled materials in the hoppers considered under the filling phase (i.e., less than 20 kPa), typical values for Young's modulus of granular agricultural materials used in silo design have been measured to be in the range of 0.3-1.7 MPa [43,44]. Therefore, an upper bound of 2 MPa was used and the variations of OPF and RPF values were calculated. In this regard, there were no significant changes. This result was expected in accordance with previous studies [18,39].

The effect of unit weight (γ) of ensiled materials was examined by considering two more unit weight. The changes of OPF and RPF values were again negligible. **Table 3** summarizes the corresponding results. Therefore, the Young's modulus and the unit weight of bulk solids were not taken into account for further investigations. But the effects of Poisson's ratio (ν) of ensiled materials, the wall friction coefficient (μ) and the hopper dimensions on OPF and RPF values were fully explored.

Table 3. The effect of Young's modulus and unit weight of bulk solids on OPF and RPF values.

Variable	Value	*e/D*							
		0.1		0.2		0.3		0.416	
		RPF	OPF	RPF	OPF	RPF	OPF	RPF	OPF
E(MPa)	0.55	0.92	1.08	0.83	1.14	0.74	1.20	0.62	1.23
	2	0.93	1.08	0.85	1.15	0.76	1.20	0.64	1.21
	4900	0.92	1.08	0.84	1.16	0.75	1.21	0.63	1.24
γ(kN/m^3)	9800	0.92	1.08	0.83	1.14	0.74	1.20	0.62	1.23
	14700	0.92	1.08	0.83	1.14	0.74	1.19	0.62	1.23

The importance of wall friction coefficient has been mentioned in some previous researches [18,30] and is considered as a key parameter in European Standard formula [36]. For these parameters, three practical values were picked as follows: for wall friction coefficient values of 0.2, 0.35 and 0.5, representing smooth to rough surfaces, and for Poisson's ratio values of 0.25, 0.3 and 0.35 [43,44]. In each case, the relevant parameter was changed, while the other basic material parameters were kept unchanged.

In order to explore the effect of hopper geometry, two other hoppers with aspect ratios (height to diameter ratio H/D) of 0.5 and 0.67 were also analyzed (**Figure 8**). Keeping almost the same height, the largest and the smallest hoppers cross sections were selected in a way to make similar eccentricity ratios of sample hopper (**Figure 1**). In this way, a practical range of aspect ratios for steel hoppers is covered in the current research [27,29,31,45–48].

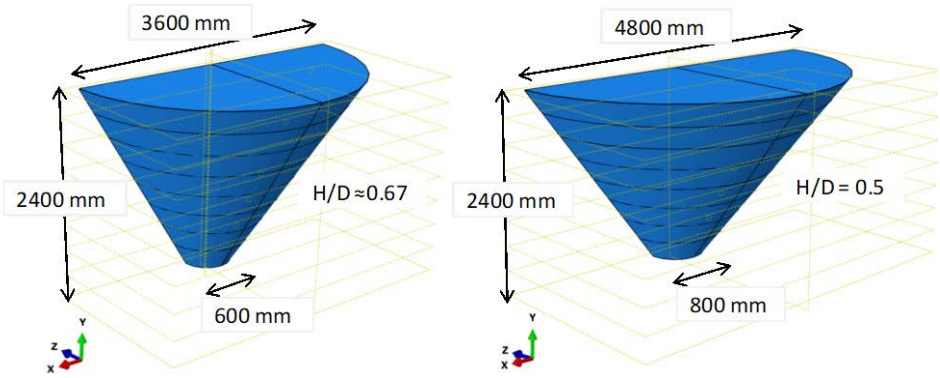

Figure 8. Hoppers dimensions with aspect ratio of ≈0.67 (left) and 0.5 (right).

The detailed results of the numerical analyses are summarized in **Table 4**. In this table, an additional column represents the elevation at which the peak normal pressures occurred for each case. This elevation is the same for Left and Right guide lines. The results of **Table 4** from a general point of view indicate that:

1) As the wall friction coefficient reduces, the values of OPF and RPF experience a decrease and an increase, respectively;

2) As the Poisson's ratio increases, the OPF values decrease and the RPF values increase. The OPF values are less sensitive to Poisson's ratio when compared with the RPF values;

3) As the eccentricity grows, the effects of both wall friction coefficient and Poisson's ratio on OPF and RPF values increase. Moreover, the variations of these two factors with Poisson's ratio when larger value of wall friction coefficient is used are more traceable;

4) As the hopper aspect ratio decreases, the RPF values also decrease while the results don't show a certain trend for OPF values. For hoppers with aspect ratio of 0.67 and 0.5, in transition from 0.3 to 0.416 for the amount of eccentricity ratio, the OPF values may increase or decrease;

5) As the wall friction coefficient increases, the elevation of peak pressure occurrence also increases. The amount of Poisson's ratio makes negligible effect on this issue. But lowering the hopper aspect ratio decreases the corresponding peak pressure elevation;

6) Considering all parameters studied in the current research, the variations in OPF values are less than the RPF values.

The values of OPF and RPF shown in **Table 4** expand the perspective that how the outlet eccentricity would influence the peak normal pressures. In order to compare the pressure predictions for concentric hoppers by progressive filling method with the formula of European Standard the following section is presented.

Table 4. Parametric study on OPF and RPF values.

NO.	*H*/*D*	μ	v	*e*/*D*								Corresponding elevation from outlet (*z*/*H*)
				0.1		0.2		0.3		0.416		
				RPF	OPF	RPF	OPF	RPF	OPF	RPF	OPF	
1	1	0.20	0.25	0.95	1.05	0.90	1.07	0.84	1.10	0.77	1.11	0.21
2	1	0.20	0.30	0.95	1.05	0.90	1.07	0.85	1.09	0.78	1.11	0.21
3	1	0.20	0.35	0.95	1.04	0.90	1.07	0.85	1.08	0.78	1.10	0.21
4	1	0.35	0.25	0.93	1.06	0.84	1.11	0.76	1.15	0.66	1.18	0.29
5	1	0.35	0.30	0.93	1.06	0.85	1.11	0.77	1.14	0.68	1.17	0.29
6	1	0.35	0.35	0.94	1.05	0.86	1.10	0.78	1.13	0.69	1.15	0.29
7	1	0.50	0.25	0.91	1.08	0.81	1.14	0.70	1.20	0.58	1.23	0.29
8	1	0.50	0.30	0.92	1.08	0.83	1.14	0.74	1.20	0.62	1.23	0.29
9	1	0.50	0.35	0.93	1.07	0.86	1.14	0.79	1.20	0.69	1.24	0.29
10	0.67	0.20	0.25	0.92	1.06	0.83	1.11	0.74	1.14	0.65	1.14	0.19
11	0.67	0.20	0.30	0.92	1.06	0.84	1.11	0.76	1.13	0.67	1.13	0.19
12	0.67	0.20	0.35	0.93	1.06	0.86	1.10	0.78	1.12	0.69	1.11	0.17
13	0.67	0.35	0.25	0.89	1.09	0.78	1.16	0.66	1.20	0.52	1.20	0.2
14	0.67	0.35	0.30	0.90	1.07	0.79	1.15	0.68	1.18	0.55	1.18	0.2
15	0.67	0.35	0.35	0.92	1.08	0.83	1.13	0.73	1.18	0.62	1.19	0.19
16	0.67	0.50	0.25	0.88	1.11	0.76	1.19	0.62	1.25	0.47	1.27	0.28
17	0.67	0.50	0.30	0.90	1.10	0.80	1.18	0.68	1.23	0.55	1.26	0.28
18	0.67	0.50	0.35	0.91	1.07	0.82	1.14	0.72	1.18	0.61	1.21	0.28
19	0.5	0.20	0.25	0.91	1.10	0.80	1.15	0.68	1.18	0.56	1.16	0.13
20	0.5	0.20	0.30	0.92	1.09	0.82	1.14	0.71	1.16	0.59	1.14	0.13
21	0.5	0.20	0.35	0.92	1.07	0.83	1.12	0.74	1.14	0.64	1.11	0.13
22	0.5	0.35	0.25	0.88	1.11	0.74	1.20	0.60	1.23	0.45	1.21	0.14
23	0.5	0.35	0.30	0.90	1.10	0.78	1.17	0.66	1.20	0.53	1.19	0.14
24	0.5	0.35	0.35	0.91	1.08	0.82	1.13	0.71	1.16	0.59	1.16	0.16
25	0.5	0.50	0.25	0.87	1.12	0.74	1.21	0.59	1.25	0.44	1.26	0.16
26	0.5	0.50	0.30	0.88	1.08	0.76	1.15	0.63	1.19	0.49	1.20	0.19
27	0.5	0.50	0.35	0.91	1.06	0.80	1.11	0.69	1.14	0.56	1.14	0.19

3.3 Comparison of progressive filling method with EC 1991-4:2006

In the current section the normal pressures predicted by FEM and the European Standard [36] are compared. Three concentric hoppers with three values of wall friction coefficient (similar to the parametric study) were considered. A typical value of 0.3 was picked for the bulk solid Poisson's ratio. According to the Standard [36], there is a distinction between the value of wall friction coefficient for steep and shallow hoppers. Accordingly, a

steep hopper, in which the solid slides down the inclined hopper wall when the silo is filled, is treated by using fully mobilized wall friction. On the other hand, in shallow ones, too low of a slope or high friction causes the solid not to slide down the inclined hopper wall when the silo is filled and hence wall friction not being fully mobilized. If $\beta < \beta_{cr}$ (Equation (1)) the hopper is deemed to be steep and the hopper wall is fully mobilized, otherwise the effective hopper wall friction coefficient (Equation (2)) may be used:

$$tan\,\beta_{cr} = \frac{1-K}{2\tan\varphi_w} \quad and \quad \mu = \tan\varphi_w \tag{1}$$

$$\mu_{eff} = \frac{1-K}{2\tan\beta} \tag{2}$$

Where β is the hopper half angle, φ_w is the friction angle between the wall and the particulate solid. In the current paper, the wall friction coefficient (μ) was directly used instead in all parts. K is the lateral pressure ratio on vertical wall with a typical value between 0.4 and 0.6 [1,36] and was calculated by $K=\nu/(1-\nu)$ [3,18,39] for filling state. **Table 5** shows the parameters used for pressure calculations and the distinction made between steep and shallow hopper in accordance with its hopper half angle and wall friction coefficient.

Table 5. Values used in the European Standard [36] formula for pressure calculations in hoppers.

NO.	H/D	μ (FEM)	ν	K	β°	β_{cr}°	Steep/Shallow	μ_{eff} or μ
1	1	0.20	0.30	0.43	23	54.9	Steep	0.20
2	1	0.35	0.30	0.43	23	39.2	Steep	0.35
3	1	0.50	0.30	0.43	23	29.7	Steep	0.50
4	0.67	0.20	0.30	0.43	32	54.9	Steep	0.20
5	0.67	0.35	0.30	0.43	32	39.2	Steep	0.35
6	0.67	0.50	0.30	0.43	32	29.7	Shallow	0.46
7	0.5	0.20	0.30	0.43	39.8	54.9	Steep	0.20
8	0.5	0.35	0.30	0.43	39.8	39.2	Shallow	0.34
9	0.5	0.50	0.30	0.43	39.8	29.7	Shallow	0.34

The normal pressures (P) on the hopper wall is recommended to be evaluated using the same relationships in both kind of hoppers, but adopting an effective hopper wall friction coefficient (μ_{eff}) in shallow ones [36]:

$$P = F_f\,(\frac{\gamma h_h}{n-1})\left\{(\frac{y}{h_h}) - (\frac{y}{h_h})^n\right\} \tag{3}$$

$$n = 2(1-b)\mu\cot\beta \tag{4}$$

$$F_f = 1 - \frac{b}{1-\frac{\tan\beta}{\mu}} \tag{5}$$

Where F_f is the hopper pressure ratio for filling, n is an exponent given by Equation (4) and b is an empirical coefficient with recommended value of 0.2. Also, h_h is the vertical height between the hopper apex and the transition and y is the vertical coordinate upwards from hopper apex (see **Figure 9**).

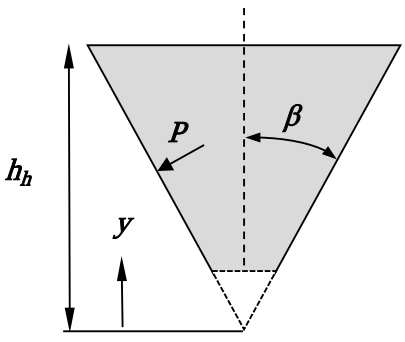

Figure 9. Illustration of the notations used in Equation (3).

Figure 10 represents the predicted normal pressures distribution by both methods. Due to similar effective hopper wall friction coefficient obtained for hopper with aspect ratio of 0.5 (see **Table 5**), the Standard [36] formula results in the same curve for μ= 0.35 and μ= 0.5. There is a good agreement between the predicted results. With this respect it may be possible to use the calculated OPF and RPF values (see **Table 4**) in conjunction with the European Standard formula [36] for concentric hoppers to capture the hopper eccentricity effects.

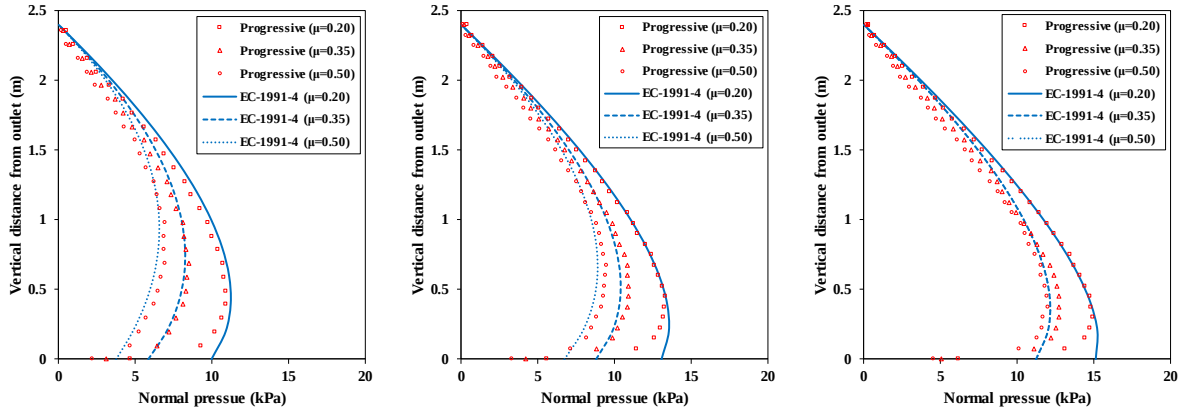

Figure 10. Progressive filling method and European standard [36] normal pressure distribution for concentric hoppers, for the following hoppers aspect ratios: (a) ≈1; (b) ≈0.67 and (c) 0.5.

4. Conclusions

The main conclusions from the numerical analyses of hoppers with different values of outlet eccentricities can be drawn as follows:

1) It has been shown that the effect of outlet eccentricity in hopper body, results in asymmetry of pressures exerted on hopper wall. The results show an increase in the normal pressures of shallow side compared with the steep side of eccentric hopper. In order to quantify this asymmetry, OPF and RPF were introduced to determine the amount of peak pressure variations with respect to that of concentric hopper.

2) It was concluded that due to small strains [42] and low pressure levels in the filling phase in hoppers, the elastic behavior is dominant and plastic parameters have minor effects. This is consistent with the little effect of the adopted constitutive model for stored solids on the filling pressures [2,3,18,41]. Therefore, in the parametric study the plastic parameters were kept unchanged. In addition, it was found that the unit weight and Young's modulus of bulk solids have minor effects on OPF and RPF values.

3) A full parametric study considering three different hoppers, three different values for wall friction coefficient and the Poisson's ratio was carried out. As reported values in **Table 4** show, the wall friction coefficient has an essential effect on OPF and RPF values. The OPF values are less sensitive to Poisson's ratio when compared with the RPF values. As the eccentricity grows, the effects of both wall friction coefficient and Poisson's ratio on OPF and RPF values increase. Moreover, a reduction in the hopper aspect ratio decrease the RPF values while the OPF values don't follow a certain trend. As a general rule, the OPF values show less sensitivity as compared to RPF values to these parameters' changes.

4) Finally, the comparison between the FEM and the European Standard formula [36] for concentric hoppers showed a close agreement of normal pressures prediction by these methods. Consequently, it may be possible to use the calculated OPF and RPF values of this paper in conjunction with the European Standard formula for axisymmetric hoppers in order to capture the hopper eccentricity effects.

5. References

[1] Ding S, Rotter JM, Ooi JY, Enstad G. Development of normal pressure and frictional traction along the walls of a steep conical hopper during filling. Thin-walled Structures. 2011;49(10):1246-1250.

[2] Chen JF, Yu SK, Ooi JY, Rotter JM. Finite-element modeling of filling pressures in a full-scale silo. Journal of Engineering Mechanics. 2001;127(10):1058-1066.

[3] Ding S, Rotter JM, Ooi JY, Enstad G, Xu D. Normal pressures and frictional tractions on shallow conical hopper walls after concentric filling: predictions and experiments. Chemical Engineering Science. 2013;89:264-272.

[4] Rotter JM, Brown CJ, Lahlouh EH. Patterns of wall pressure on filling a square planform steel silo.

Engineering Structures. 2002;24(2):135-150.
[5] Holst JM, Ooi JY, Rotter JM, Rong GH. Numerical modeling of silo filling. I: continuum analyses. Journal of Engineering Mechanics. 1999;125(1):94-103.
[6] Janssen HA. Experiments on grain pressure in silo cells. Journal of the Association of German Engineers. 1895; 39:1045-1049 (in German).
[7] Enstad G. On the theory of arching in mass flow hoppers. Chemical Engineering Science. 1975;30(10):1273-1283.
[8] McLean AG, Arnold PC. Prediction of cylinder flow pressures in mass-flow bins using minimum strain energy. J. Eng. Ind. 1976;98:1370–1374.
[9] Walker DM. An approximate theory for pressures and arching in hoppers. Chemical Engineering Science. 1966;21(11):975-997.
[10] Walters JK. A theoretical analysis of stresses in axially-symmetric hoppers and bunkers. Chemical Engineering Science. 1973;28(3):779-789.
[11] Nedderman RM. Statics and kinematics of granular materials. Cambridge University Press; 2005.
[12] Horne RM, Nedderman RM. Stress distribution in hoppers. Powder Technology. 1978;19(2):243-254.
[13] Jenike AW, Johanson JR, Carson JW. Bin loads—part 4: funnel-flow bins. J. Eng. Ind. 1973;95:13–16.
[14] Jenike AW, Johanson JR, Carson JW. Bin loads—part 3: mass-flow bins. J. Eng. Ind. 1973;95:6–12.
[15] Jenike AW, Johanson JR, Carson JW. Bin loads—part 2: concepts. J. Eng. Ind. 1973;95:1–5.
[16] Jenike AW, Johanson JR. On the theory of bin loads. J. Eng. Ind. 1969;91:339–344.
[17] Ding S, Enstad GG, De Silva SR. Development of load on a hopper during filling with granular material. Particulate Science and Technology. 2003;21(3):259-270.
[18] Ooi JY, Rotter JM. Elastic predictions of pressures in conical silo hoppers. Engineering Structures. 1991;13(1):2-12.
[19] Häussler U, Eibl J. Numerical investigations on discharging silos. Journal of Engineering Mechanics. 1984;110(6):957-971.
[20] Keiter TW, Rombach GA. Numerical aspects of FE simulations of granular flow in silos. Journal of Engineering Mechanics. 2001;127(10):1044-1050.
[21] Martinez MA, Alfaro I, Doblare M. Simulation of axisymmetric discharging in metallic silos. Analysis of the induced pressure distribution and comparison with different standards. Engineering Structures. 2002;24(12):1561-1574.
[22] Wang Y, Lu Y, Ooi JY. Numerical modelling of dynamic pressure and flow in hopper discharge using the Arbitrary Lagrangian–Eulerian formulation. Engineering Structures. 2013;56:1308-1320.
[23] Wang Y, Lu Y, Ooi JY. Finite element modelling of wall pressures in a cylindrical silo with conical hopper using an Arbitrary Lagrangian–Eulerian formulation. Powder Technology. 2014;257:181-190.
[24] Huang X, Zheng Q, Yu A, Yan W. Shape optimization of conical hoppers to increase mass discharging rate. Powder Technology. 2020;361:179-189.
[25] Jin W, Stickel JJ, Xia Y, Klinger J. A review of computational models for the flow of milled biomass Part II: Continuum-mechanics models. ACS Sustainable Chemistry & Engineering. 2020;8(16):6157-6172.
[26] Pardikar K, Wassgren C. Predicting the critical outlet width of a hopper using a continuum finite element method model. Powder Technology. 2019;356:649-660.
[27] Ayuga F, Guaita M, Aguado PJ, Couto A. Discharge and the eccentricity of the hopper influence on the silo wall pressures. Journal of Engineering Mechanics. 2001;127(10):1067-1074.
[28] Guaita M, Couto A, Ayuga F. Numerical simulation of wall pressure during discharge of granular material from cylindrical silos with eccentric hoppers. Biosystems Engineering. 2003;85(1):101-109.
[29] Ramírez A, Nielsen J, Ayuga F. Pressure measurements in steel silos with eccentric hoppers. Powder Technology. 2010;201(1):7-20.
[30] Vidal P, Couto A, Ayuga F, Guaita M. Influence of hopper eccentricity on discharge of cylindrical mass flow silos with rigid walls. Journal of Engineering Mechanics. 2006;132(9):1026-1033.
[31] Vidal P, Gallego E, Guaita M, Ayuga F. Finite element analysis under different boundary conditions of the filling of cylindrical steel silos having an eccentric hopper. Journal of Constructional Steel Research. 2008;64(4):480-492.
[32] Wójcik M, Enstad GG, Jecmenica M. Numerical calculations of wall pressures and stresses in steel cylindrical silos with concentric and eccentric hoppers. Particulate Science and Technology. 2003;21(3):247-258.
[33]Gallego E. Numerical simulation of loads exerted by stored materials in silos with non-elastic material models. 2006.
[34] Ding S, Ji Y, Ye S, Rotter JM, Li Q. Measurements of pressure and frictional tractions along walls of a large-scale conical shallow hopper and comparison with Eurocode 1991-4: 2006. Thin-Walled Structures. 2014;80:231-238.
[35] Dassault Systèmes Simulia. Abaqus CAE user's manual; 2012.

[36] EN 1991-4. Eurocode 1: Actions on structures - Part 4: Silos and tanks. CEN, Brussels. 2006.
[37] Zhong Z, Ooi JY, Rotter JM. The sensitivity of silo flow and wall stresses to filling method. Engineering Structures. 2001;23(7):756-767.
[38] Nielsen J. Pressures from flowing granular solids in silos. Philosophical Transactions of the Royal Society of London. Series A: Mathematical, Physical and Engineering Sciences. 1998;356(1747):2667-2684.
[39] Chen JF, Rotter JM, Ooi JY. A review of numerical prediction methods for silo wall pressures. Advances in Structural Engineering. 1999;2(2):119-135.
[40] Wang X, Yang Z, Shu X, Feng J. The static contact statuses between granular materials and flat-bottomed steel silos. Powder Technology. 2013;235:1053-1059.
[41] Ooi JY, Rotter JM. Elastic and plastic predictions of the storing pressures in conical hoppers. In:Third International Conference on Bulk Materials, Storage, Handling and Transportation: Preprints of Papers. Institution of Engineers, Australia. 1989.p. 203.
[42] Rombach G. Martinez J. Introduction and scope. In: C.J. Brown, J. Nielsen (Eds.), Silos Fundam. Theory, Behav. Des. E & FN Spon, London, 1998. p. 471–475.
[43] Moya M, Aguado PJ, Ayuga F. Mechanical properties of some granular agricultural materials used in silo design. International Agrophysics. 2013;27(2):181–193.
[44] Ramírez A, Moya M, Ayuga F. Determination of the mechanical properties of powdered agricultural products and sugar. Particle & Particle Systems Characterization. 2009;26(4):220-230.
[45] Wójcik M, Sondej M, Rejowski K, Tejchman J. Full-scale experiments on wheat flow in steel silo composed of corrugated walls and columns. Powder Technology. 2017;311:537-555.
[46] Gurfinkel G, Pecknold DA. Conical hoppers of tall steel tanks: Case history of failure and repair. Journal of Performance of Constructed Facilities. 1997;11(2):50-57.
[47] Gurfinkel G. Collapse and repair of tall concrete silos with suspended steel hopper. Journal of Performance of Constructed Facilities. 1989;3(4):243-264.
[48] Gurfinkel G. Tall steel tanks: failure, design, and repair. Journal of Performance of Constructed Facilities. 1988;2(2):99-110.